This paper originally appeared in *Proceeding of Information Processing in Medical Imaging 2005 (IPMI 2005)*, Glenwood Springs, Colorado
http://www.springer.de/comp/lncs/index.html

Coupled shape distribution-based segmentation of multiple objects *

Andrew Litvin[1] and William C. Karl[1]

Boston University,
Boston, Massachusetts
{litvin,wckarl}@bu.edu

Abstract. In this paper we develop a multi-object prior shape model for use in curve evolution-based image segmentation. Our prior shape model is constructed from a family of shape distributions (cumulative distribution functions) of features related to the shape. Shape distribution-based object representations possess several desired properties, such as robustness, invariance, and good discriminative and generalizing properties. Further, our prior can capture information about the interaction between multiple objects. We incorporate this prior in a curve evolution formulation for shape estimation. We apply this methodology to problems in medical image segmentation.

1 Introduction

The use of prior information about shape is essential when image intensity alone does not provide enough information to correctly segment objects in a scene. Such cases arise due to the presence of clutter, occlusion, noise, etc. In this work we concentrate on curve evolution-based image segmentation approaches [1] and prior shape models matched to this framework. In a typical curve evolution scheme, the regions of interest in the image (i.e. the shapes or objects) are represented by non-self-intersecting closed contours. Curve evolution methods allow convenient handling of object topology, efficient implementation, and possess variational and associated probabilistic interpretations. In a typical curve

* This work was partially supported by AFOSR grant F49620-03-1-0257, National Institutes of Health under Grant NINDS 1 R01 NS34189, Engineering research centers program of the NSF under award EEC-9986821. The MR brain data sets and their manual segmentations were provided by the Center for Morphometric Analysis at Massachusetts General Hospital and are available at http://www.cma.mgh.harvard.edu/ibsr/.

evolution implementation, the shape-capturing curve is evolved under the combined action of two classes of forces: those dependent on the observed image data (data-dependent forces) and those reflecting prior knowledge about the segmented shape or boundary (regularizing forces). This work is focused on the development of shape models suitable for such prior shape force terms in curve evolution.

Desirable qualities in a shape-based prior include invariance with respect to transformations such as scale, translation, and rotation, independence from knowledge of correspondence, robustness of the resulting solution to initialization, the ability to generate the prior model from training data, and subsequent robustness to small training set size. Shape distributions have been used in the computer graphics community [14] to characterize shapes and, more recently, have been successfully applied to shape classification problems. They were shown to possess the desired properties of robustness, invariance, and flexibility. To date, however, shape distributions have not been used in an estimation context.

In this work we develop a novel multi-object prior based on such shape distributions for use in estimation. We then present a method to use this prior in curve evolution-based segmentation problems. Finally, we suggest the promise of this prior for challenging medical image segmentation tasks through an example. In our formulation, the shape prior is constructed by designing a shape similarity measure penalizing the difference between shape distributions extracted from boundary curves under comparison.

In Section 2 we give an overview of existing shape modeling approaches and the motivations behind our technique. In Section 3 we review the curve evolution framework and introduce the shape distribution concept. Section 4 presents our experimental results and Section 5 concludes this paper.

2 Prior work

Different approaches have been proposed for the inclusion of prior information in deformable curve-based image segmentation. The most common regularization method for curve evolution penalizes a quantity such as total curve length or object area [1, 10]. Such "generic" penalties are stationary along the curve, in that every point on the boundary experiences the same effect. Such priors can remove object protrusions and smooth salient object detail when the boundary location is not well supported by the observed data, since they seek objects with short boundaries or small area.

Deformable template approaches construct prior models based on allowable deformations of a template shape. Some approaches are based on representing and modeling shape as a set of landmarks (see [5, 4] and references therein). Other approaches use principal component analysis based on parameterized boundary coordinates or level-set functions to obtain a set of shape expansion functions [20, 22] that describe the subspace of allowable shapes. Still other approaches construct more complex parametric shape representations, such as the MREP approach in [16], or deformable atlas based approach in [3]. These meth-

ods are effective when the space of possible curves is well covered by the modeled template deformations as obtained through training data, but may not generalize well to shapes unseen in the training set.

Motivated by such limitations in existing approaches and by the representational richness of the ideas in [24, 14], we propose construction of a shape prior based on an energy which penalizes the difference between a set of feature *distributions* of a given curve and those of a prior reference set. Such prior shape distributions capture the existence of certain visual features of a shape regardless of the location of these features. Shape distributions have been successfully applied to shape classification tasks (e.g. [8, 14] and references therein), and these results indicate that shape distributions are robust, invariant, flexible shape representations with good discriminative properties. In this work, we apply such shape distribution-based models to problems of boundary estimation in medical imaging, suggesting their potential.

Simultaneous multiple object segmentation is an important direction of research in medical imaging. The positions of segmented parts are often highly correlated and can be used to further constrain the resulting boundary estimation. In [23, 18] the authors extend the PCA shape model to constrain multiple object locations. In [6], a PDM model was extended to model multiple shapes. In [7, 15] the authors mutually constrained shapes by penalizing quantities such as area of overlap between different objects. These approaches do not include shape specific information regarding the different objects. Our approach shares a common idea with [13], where the concept of a force histogram was used to characterize shapes. In [13] histogram-based descriptors were used solely in discrimination while our focus is to use similar descriptors in estimation problems.

In [11], the authors present preliminary results on constructing shape distribution-based shape models for single objects. This paper improves upon and extends this technique to the multiple object case. In contrast to existing approaches, this model attempts to directly encode properties of a class of shapes (versus simply penalizing points of high curvature), yet does not depend on the specific embedding of a shape, and thus generalizes well to unseen objects. As another major contribution, analytical expressions for energy minimizing gradient curve flows are derived, providing useful insights as well as efficient curve evolution implementation. Our approach seems to provide an interesting alternative shape prior, well matched to curve evolution approaches, with promise for challenging segmentation problems.

3 General formulation and shape distribution prior

3.1 Segmentation by energy minimization based on curve evolution.

First, we review the overall approach of segmentation in a curve evolution framework based on energy minimization. We assume that each object (shape) in the image is defined by a separate closed curve. An energy functional is defined for each object (in contrast to the multi-phase approach in [21]) and each boundary

is evolved to minimize the overall energy. For a single object, then, the solution curve C^* is sought as:

$$C^* = \underset{C}{\operatorname{argmin}}\ E(C) \tag{1}$$

The energy $E(C)$ consists of a data term and a shape prior term:

$$E(C) = E_{data}(C) + \alpha E_{prior}(C) \tag{2}$$

The data term E_{data} favors the fidelity of the solution to the image data. This term is sensor and application specific. In this paper we use two definitions of E_{data}: the bimodal image energy in [2] and the information theoretic energy in [9]. Our contribution is focused on the shape prior term E_{prior}, which we base on the concept of shape-distributions, discussed in Sec. 3.2. The positive scalar α is a regularization parameter that balances the strength of the prior and data.

The gradient curve flow minimizing (2) can be found using variational approaches or shape-gradient approaches. In this work we utilize variational approaches. The curve is then evolved according to the gradient curve flow $dC/dt = -\nabla E(C)$, were t is an artificial time parameter. We implement the curve evolution via the level-set framework [17]. This framework is very general, and our prior term can be coupled with many existing data terms (ex. [2, 9]). In the multi-object case the simultaneous evolution of multiple boundaries effectively minimizes an energy which is a sum of terms (2) corresponding to the individual objects.

3.2 The Shape Distribution Concept

Distributions of features measured over shapes in a uniform way, are called shape distributions [14]. As shown by recent shape classification experiments [14], such shape distributions can capture the intuitive similarity of shapes in a flexible way while being robust to a small sample size and invariant to object transformation.

In a continuous formulation, shape distributions are defined as sets of cumulative distribution functions (CDFs) of feature values (one distribution per collection of feature values of the same kind) measured along the shape boundary or across the shape area. Joint CDFs of multiple features can also be considered, although in this work we only consider one-dimensional distributions. An illustrative example of the shape distribution idea is shown in Figure 1, using boundary curvature as the feature. We define the shape distribution for a class or set of shapes as an average of the cumulative distribution functions corresponding to the individual shapes in the group. This approach is equivalent to combining feature value representations (continuous functions or discrete sets of values) measured on individual shapes into a single set and then defining the overall CDF of the resulting set.

We will call a set of feature values extracted from a shape a "feature class". In the example of Figure 1 the feature class is boundary curvature. Separate feature classes capturing different characteristics of shapes can be combined in a single framework, creating a more versatile prior. We distinguish two types

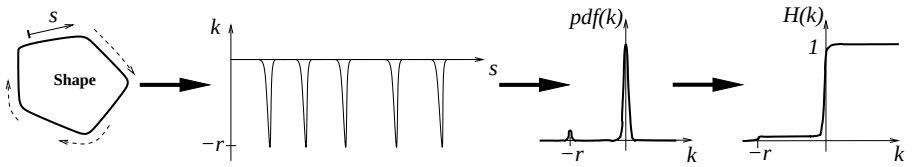

Fig. 1. An example of constructing a shape distribution for a curve (left) based on curvature $\kappa(s)$ measured along the boundary (second graph). Third and fourth graphs show the sketches of $pdf(\kappa)$ and cumulative distribution function $H(\kappa)$ of curvature respectively. Note the invariance of $H(\kappa)$ with respect to the choice of the initial point of arc-length parameterization.

of feature classes. For the first type of feature, which we term autonomous, the values for a particular curve are computed with reference only to the curve itself. For the second type of feature, which we term directed, the feature values are computed with reference to the curves of other objects. By incorporating directed feature classes into our shape models we provide a mechanism for modeling the relationships between different objects in a scene and, thus, create a framework for multi-object segmentation.

3.3 A prior energy based on shape distributions

We now introduce our formulation of the shape prior in the continuous domain. Let $\Phi \in \Omega$ be a continuously defined feature (e.g. curvature along the length of a curve), and let λ be a variable spanning the range of values Λ of the feature. Let $H(\lambda)$ be the CDF of Φ:

$$H(\lambda) = \frac{\int_\Omega h\left\{\Phi(\Omega) < \lambda\right\} d\omega}{\int_\Omega d\omega} \tag{3}$$

where $h(x)$ is the indicator function, which is 1 when the equality is satisfied and 0 otherwise.

We define the prior energy $E_{prior}(C)$ for the boundary curve C in (2) based on this shape distribution as:

$$E_{prior}(C) = \sum_{i=1}^{M} w_i \int_\Lambda \left[H_i^*(\lambda) - H_i(C,\lambda)\right]^2 d\lambda \tag{4}$$

where M is the number of different distributions (i.e. feature classes) being used to represent the object, $H_i(C,\lambda)$ is the distribution function of the i^{th} feature class for the curve C, and the non-negative scalar weights w_i balance the relative contribution of the different feature distributions. Prior knowledge of object behavior is captured in the set of target distributions $H_i^*(\lambda)$. These target distributions H_i^* can correspond to a single prior shape, an average derived from a group of training shapes, or can be specified by prior knowledge (e.g.

the analytic form for a primitive, such as a square). In practice, we compute the feature values, the corresponding shape distributions, and evolution forces dC/dt by discretizing curves and their properties through uniform sampling.

We use three specific feature classes in our experiments in this work, which we define below and illustrate in Figure 2.

- **Feature class # 1.** Inter-node Distances (Autonomous feature type). The feature value set $\{F\}$ consists of the normalized distances between nodes of the discrete curve.

$$\{F\} = \frac{\{d_{ij} \mid (i,j) \in S\}}{\text{mean}\Big(\{d_{ij} \mid (i,j) \in S\}\Big)} \tag{5}$$

  The set S defines the subset of internodal distances used in the feature. For $(a,b) \in [0,1]$, $S_{(a,b)}$ defines such subset of nodes in a multi-scale way: $\{(i,j) \mid (j-i) * ds/L \in [a,b]\}$, where a and b are the lower and upper bounds of the interval respectively; ds is the distance between neighboring boundary nodes and L is the total boundary length. In the experiments presented in this paper we used 4 different, non-overlapping intervals. Note that the features defined above are invariant to shape translation, rotation and scale.
- **Feature class # 2.** Multiscale curvature (Autonomous feature type). The feature value set $\{F\}$ consists of the collection of angles between nodes of the discrete curve.

$$\{F\} = \{\angle_{i-j,i,i+j} \quad (i,j) \in S\} \tag{6}$$

  where $\angle(ijk)$ is the angle between nodes i, j, and k. Again, the set S defines the subset of internodal angles used in the feature and again we used S in a multi-scale way, as described in Feature class #1. Similar invariance properties hold for this feature class by construction.
- **Feature class # 3.** Relative inter-object distances. (Directed feature type) The set $\{F\}$ consists of the collection of shortest signed distances between each node of C and the boundary of object Γ (negative for nodes of C inside Γ). These distances are normalized by the average radius of Γ with respect to its center of mass. This feature class encodes the relative position of C with respect to Γ. Note that the prior defined using this feature class provides a descriptor richer than those in penalty based approaches in [7, 15], while being less restrictive than a PCA based prior. Again, this feature is invariant to translation, rotation and scale applied to the pair of shapes C and Γ.

3.4 Gradient flow computation

In order to use the energy in (4) as a prior in a curve evolution context we must be able to compute the curve flow that minimizes it. For simplicity, we consider here an energy defined on just a single feature class. Since (4) is additive in the different feature classes, minimizing flows for single individual feature classes can

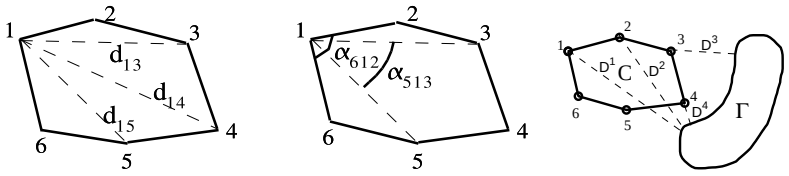

Fig. 2. Feature value sets used in this work illustrated for a curve C discretized using 6 nodes. Feature class #1 (left): interpoint distances $\{d_{13}..d_{15}\}$. Feature class #2 (center): interpoint angles $\{\alpha_{-1,1,2}..\alpha_{-n,1,n}\}$ $(n = 2)$ are shown. Feature class #3 (right): feature set values for curve C are defined as shortest signed distances from the curve Γ to nodes of the curve C.

be added with the corresponding weights to obtain the overall minimizing flow. The energy for a single feature class is given by:

$$E(C) = \int \Big[H^*(\lambda) - H(C,\lambda)\Big]^2 d\lambda \tag{7}$$

Because the energy depends on the whole curve in non-additive way, the minimizing flow at any location on the curve also depends on the whole curve, and not just the local curve properties.

The minimizing flow and its computation will, of course, depend on the specifics of the feature classes chosen. In [11], a numerical scheme was proposed to estimate the flow. Such a scheme can be employed for any definition of the feature class; although, it is computationally expensive. Here we introduce an efficient approach to analytically compute the minimizing flows for the feature classes presented previously using a variational framework. The resulting flows guarantee reduction of the energy functionals (7).

Due to the space constraints we only briefly outline the steps required to derive the flows and present final results for our specific feature classes.

1. Find the Gâteaux semi-derivative of the energy in (7) with respect to a perturbation β. Using the definition of the Gâteaux semi-derivative, the linearity of integration, and the chain rule we obtain

$$\mathcal{G}(E,\beta) = 2\int \Big[H^*(\lambda) - H(\Gamma,\lambda)\Big]\ \mathcal{G}\Big[H(\gamma,\lambda),\beta\Big]\, d\lambda \tag{8}$$

2. If the Gâteaux semi-derivative of a linear functional f exists, then according to the Rietz representation theorem, it can be represented as

$$\mathcal{G}(f,\beta) =< \nabla f, \beta > \tag{9}$$

were ∇f is the gradient flow minimizing the functional f. Therefore, we must find the boundary functional representation $\nabla H(\Gamma,\lambda)$ for the feature such that $\mathcal{G}\Big[H(\Gamma,\lambda),\beta\Big] =< \nabla H(\Gamma,\lambda), \beta >$.

3. The overall flow minimizing (7) is then given by

$$\nabla E = 2 \int \Big[H^*(\lambda) - H(\Gamma, \lambda) \Big] \nabla H(\Gamma, \lambda) d\lambda \tag{10}$$

A detailed derivation of the gradient flows for the three features used in this work can be found in the technical report [12]. We simply summarize those results here. For feature class #1 the minimizing flow is given by:

$$\nabla E(\Gamma)(s) = 2 \int_{t \in S} \boldsymbol{n}(s) \cdot \frac{\boldsymbol{\Gamma}(s,t)}{|\boldsymbol{\Gamma}(s,t)|} \Big[H^*(|\boldsymbol{\Gamma}(s,t)|) - H(\Gamma, |\boldsymbol{\Gamma}(s,t)|) \Big] dt \tag{11}$$

where Γ is the parameterized curve as a function of arc length $\{X(s), Y(s)\}$ with $s \in \{0, 1\}$, $\boldsymbol{\Gamma}(s,t)$ is a vector with coordinates $\{X(t) - X(s), Y(t) - Y(s)\}$, and $\boldsymbol{n}(s)$ is the outward normal at $\{X(s), Y(s)\}$. The flow at each s is an integral over the curve, indicating the non-local dependence of the flow. The expression under the integral can be interpreted as a force acting on a particular pair of locations on the curve, projected on the normal direction at s.

For feature class #2, the minimizing flow is given by

$$\begin{aligned} \nabla E(\Gamma)(s) = \\ - \int_{t \in S} \Bigg[\left\{ \begin{array}{ll} \frac{\cos(\beta)\cos(n(s),\Gamma^+) + \cos(\gamma)\cos(n(s),\Gamma^-)}{\sin\alpha} & \text{if } \alpha \neq \pi \\ \sin(\boldsymbol{n}(s), \boldsymbol{\Gamma}^-)) & \text{otherwise} \end{array} \right\} \times \frac{a \cdot r^{(s,t)}}{bc} - \\ f^{(s-t)} \frac{\sqrt{1 - \left(\boldsymbol{n}(s-t) \cdot \frac{\boldsymbol{\Gamma}^-}{|\boldsymbol{\Gamma}^-|} \right)^2}}{|\boldsymbol{\Gamma}^-|} - f^{(s+t)} \frac{\sqrt{1 - \left(\boldsymbol{n}(s+t) \cdot \frac{\boldsymbol{\Gamma}^+}{|\boldsymbol{\Gamma}^+|} \right)^2}}{|\boldsymbol{\Gamma}^+|} \Bigg] \times \\ \Big[H^*(\alpha(s,t)) - H(\Gamma, \alpha(s,t)) \Big] dt \end{aligned} \tag{12}$$

where $r^{(s,t)}$ and $f^{(s+t)}$ take values -1 and 1 and indicate the sign of change of the angle $\alpha(s,t) = \angle(\boldsymbol{\Gamma}^-, \boldsymbol{\Gamma}^+)$ with respect to along-the-normal perturbation of the point $\Gamma(s)$ and $\Gamma(s+t)$ respectively, $\boldsymbol{\Gamma}^+ = \boldsymbol{\Gamma}(s, s+t)$; $\boldsymbol{\Gamma}^- = \boldsymbol{\Gamma}(s, s-t)$; $a = |\boldsymbol{\Gamma}^+ - \boldsymbol{\Gamma}^-|$; $b = |\Gamma^-|$; $c = |\Gamma^+|$; $\beta = \angle(-\boldsymbol{\Gamma}^+, \boldsymbol{\Gamma}^- - \boldsymbol{\Gamma}^+)$; $\gamma = \angle(-\boldsymbol{\Gamma}^-, \boldsymbol{\Gamma}^+ - \boldsymbol{\Gamma}^-)$.

Finally, for feature class #3, relating the curve Γ to another object Ω, the gradient flow is given by:

$$\nabla E(\Gamma)(s) = \boldsymbol{n}(s) \cdot \boldsymbol{\nabla} \boldsymbol{D}_\Omega(s) \left[H^* \left(\frac{D_\Omega(s)}{R(\Omega)} \right) - H \left(\Gamma, \frac{D_\Omega(s)}{R(\Omega)} \right) \right] \tag{13}$$

where $D_\Omega(s)$ is value of signed distance function generated by curve Ω at the point on the curve Γ given by $\{X(s), Y(s)\}$, and $R(\Omega)$ is the mean radius of the shape Ω relative to its center of mass.

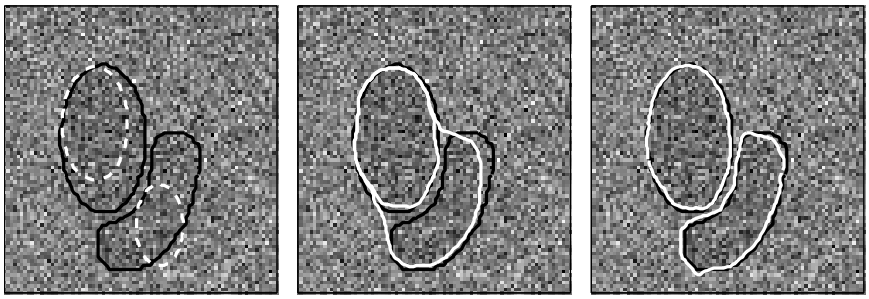

(a) (b) (c)

Fig. 3. Synthetic 2 shape example: (a) Noisy image; Solid black line shows the true objects boundaries; dashed white lines - initial boundary position; (b) Segmentation with curve length prior; (c) - Segmentation with new multiobject shape distribution prior including all three feature classes. Solid black line shows the true objects boundaries; solid white lines - final boundary.

4 Results

In this section we apply our shape distribution based prior to both a synthetic and a real example. The real data example arises in segmentation of brain MRI. We compare both single object and multi-object priors. The benefit of using a multi-object prior is expected to be greater when the object boundary is not well supported by the observed image intensity gradient or when initialization is far from the true boundary.

In the first experiment we apply our prior to a synthetic 2-object segmentation problem with very low SNR, simulating two closely positioned organs, shown in Figure 3, panel (a). Both objects in the ground truth image have the same known intensity. The background intensity is also known as in the model [2]. Gaussian IID noise (SNR= -18dB) was added to this bimodal image to form the noisy observed image. The data term E_{data} in (2) and the corresponding data-term gradient curve flow are formed according the data model in [2].

In Figure 3 we show the results obtained by segmenting this image using energy minimizing curve evolution based on two different shape priors: (b) shows the results with a curve length penalty; (c) shows the results with our multi-object shape distribution prior including all 3 feature classes. The prior target distributions for case (c) were constructed using the true objects in (a). The regularization parameter was chosen in each case to yield the subjectively best result. The curve length prior result in (b) yields an incorrect segmentation for one of the objects or leads to a collapse of one of the contours. With the directed feature class included in the segmentation functional (c), both objects can be correctly segmented since the energy term corresponding to feature class #3 effectively prevents intersection of boundaries. Segmentation errors (area based) are summarized in Table 1.

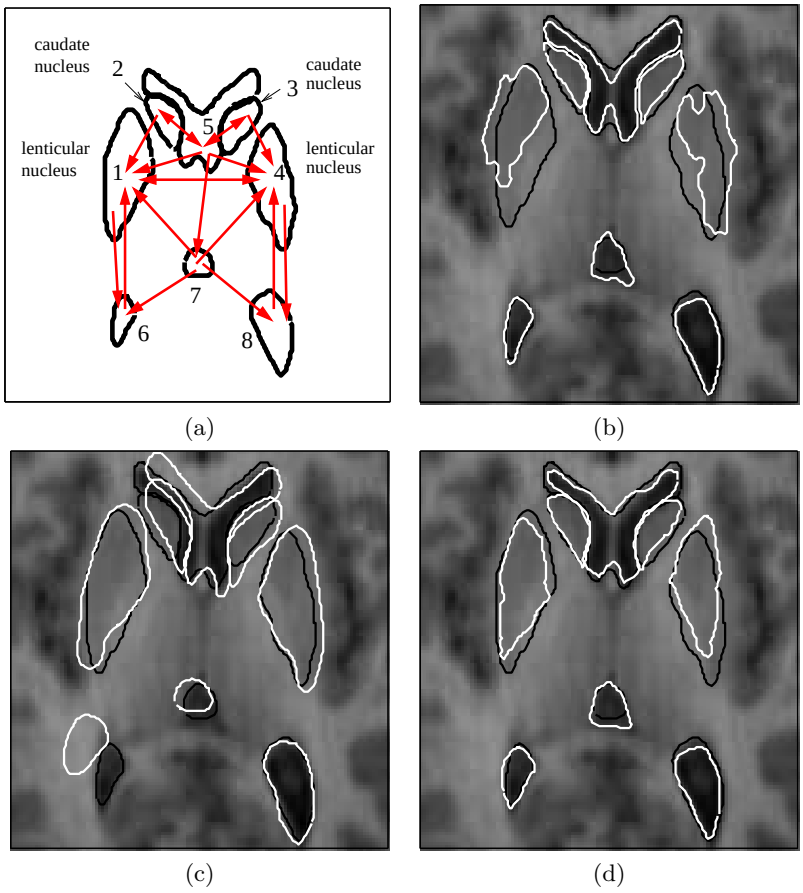

Fig. 4. Brain MRI segmentation: (a) Multiple structures and interactions used for feature class #3; (b) Segmentation with independent object curve length prior. (c) Segmentation using multiobject PCA technique in [19] (d) Segmentation with new multiobject shape distribution prior. Solid black line shows the true objects boundaries; solid white line - final segmentation boundary.

In our second example we apply our techniques to 2D MRI brain data segmentation. A data set consisting of 12 normal adult subjects was used. Manual expert segmentations of the subjects was provided and those of 11 of these subjects was used as training data to construct our shape prior. The prior was then applied to segment the data of the omitted subject. The eight numbered structures shown in Figure 4, panel (a) were simultaneously segmented. For the data dependent energy term E_{data}, we used the information theoretic approach of [9] by maximizing the mutual information between image pixel intensities and region labels (inside or outside), therefore favoring segmented regions with intensity distributions that were different from the background intensity distribution.

Table 1. Symmetric difference (area based) segmentation error. For each object the error measure is computed as a symmetric difference between final segmented region and true segmented region. The values in the table are computed as a sum of error measures for individual objects.

	Curve length	PCA method	Our method
Experiment I	1092		146
Experiment II	1090	1437	758

In Figure 4 we present our results. Panel (b) gives the segmentation with a standard curve length prior applied independently to each object. One can see that Structures 1 and 4 are poorly segmented, due to their weak image boundaries. In panel (c) we present the result given by the multi-shape PCA technique in [19] using 5 principle components defining the subspace of allowable shapes. The segmentation is sought as the shape in this subspace, optimizing the same information-theoretic criteria [9] as used with our shape prior. The usage of the same data term simplifies the comparison with our approach since only the shape model components of the method are different. One can see that structures 2,5,6, and 7 are not segmented properly due to the poor generalization by the PCA prior. Expanding the subspace by choosing 10 PCA components did not improve the result given by this method. Finally, our result is shown in panel (d). We obtain satisfactory segmentation for the structures for which PCA method failed (2,5,6,7), while performing equally well for structures 1,3,4 and 8. The choice of initialization did not significantly influence our results. Segmentation errors given in Table 1 qualitatively confirm the superior performance attained using our prior.

5 Conclusions

In this paper we present a shape distribution-based object prior for use in curve evolution image segmentation. This prior allows encoding of multi-object information. We apply a variational approach to analytically compute the energy minimizing curve flows for three feature classes. We investigate the application of our shape distribution prior to medical image segmentation involving multiple object boundaries. In our experiments we achieved the performance superior to that obtained using the traditional curve length minimization methods and a multi-shape PCA shape prior reported in the literature.

References

1. V. Caselles, R. Kimmel, and G. Sapiro, "Geodesic active contours," *International journal of computer vision*, vol. 22(1), pp. 61–79, 1997.
2. T. Chan and L. Vese, "Active contours without edges," *IEEE trans. on Image Processing*, vol. 10, no. 2, pp. 266–277, February 2001.

3. G. Christensen, "Deformable shape models for anatomy," Ph.D. dissertation, Washington University, St. Louis, US, 1994.
4. T. Cootes, C. Taylor, D. Cooper, and J. Graham, "Active shape models – their training and application," *Computer Vision and Image Understanding*, vol. 61, no. 1, pp. 38–59, 1995.
5. I. Dryden and K. Mardia, *Statistical shape analysis*. John Wiley & Sons, 1998.
6. N. Duta and M. Sonka, "Segmentation and interpretation of mr brain images: an improved active shape model," *IEEE trans. on Med. Im.*, vol. 17, no. 7, pp. 1049–1062, 1998.
7. G. Ho and P. Shi, "Domain partitioning level set surface for topology constrained multi-object segmentation," in *Proc. IEEE Intl. Symp. Biomedical Imaging*, Washington DC, US, 2004.
8. C. Y. Ip, D. Lapadat, L. Sieger, and W. Regli, "Using shape distributions to compare solid models," in *SMA '02: Proceedings of the seventh ACM symposium on Solid modeling and applications*. Saarbrcken, Germany: ACM Press, 2002, pp. 273–280.
9. J. Kim, J. W. Fisher, A. Yezzi, M. Cetin, and A. S. Willsky, "Nonparametric methods for image segmentation using information theory curve evolution," in *Proc. ICIP*, Rochester, USA, September 2002.
10. M. E. Leventon, W. E. L. Grimson, O. Faugeras, and W. M. W. III, "Level set based segmentation with intensity and curvature priors," *IEEE Workshop on Mathematical Methods in Biomedical Image Analysis Proceedings (MMBIA'00)*, pp. 4–11, 2000.
11. A. Litvin and W. C. Karl, "Using shape distributions as priors in a curve evolution framework," in *Proceedings of 2004 IEEE International Conference on Acoustic Speech and Signal Processing (ICASSP)*, Montreal, Canada, 2004.
12. ——, "Coupled shape distribution-based segmentation of multiple objects," Boston University, Boston, USA, Tech. Rep. ECE-2005-01, March 2005.
13. P. Matsakis, J. M. Keller, O. Sjahputera, and J. Marjamaa, "The use of force histograms for affine-invariant relative position description," *IEEE trans. on PAMI*, vol. 26, no. 1, pp. 1–18, 2004.
14. R. Osada, T. Funkhouser, B. Chazelle, and D. Dobkin, "Shape distributions," *ACM transactions on graphics*, vol. 21(4), pp. 807–832, 2002.
15. N. Paragios and R. Deriche, "Coupled geodesic active regions for image segmentation: A level set approach," in *European Conference in Computer Vision*, Dublin, Ireland, 2000.
16. S. M. Pizer, D. S. Fritsch, P. A. Yushkevich, V. E. Johnson, and E. L. Chaney, "Segmentation, registration, and measurement of shape variation via image object shape," *IEEE Transactions on Medical Imaging*, vol. 18(10), pp. 851–865, 1996.
17. J. Sethian, *Level set methods and fast marching methods*. Cambridge University Press, 1999.
18. A. Tsai, W. Wells, C. Tempany, G. E., and A. Willsky, "Coupled multi-shape model and mutual information for medical image segmentation," in *Proc. IPMI (Information Processing in Medical Imaging)*, Ambleside, UK, July 2003, pp. 185–197.
19. A. Tsai, W. Wells, C. Tempany, E. Grimson, and A. Willsky, "Mutual information in coupled multi-shape model for medical image segmentation," *Medical Image Analysis*, vol. 8, no. 4, pp. 429–445, 2004.
20. A. Tsai, A. Yezzi, W. Wells, C. Tempany, D. Tucker, A. Fan, W. Grimson, and A. Willsky, "Model-based curve evolution technique for image segmentation," *IEEE Conference on Computer Vision and Pattern Recognition (CVPR'01)*, 2001.

21. L. Vese and T. Chan, "A multiphase level set framework for image segmentation using the Mumford and Shah model," *International Journal of Computer Vision*, vol. 50, no. 3, pp. 271–293, 2002.
22. Y. Wang and L. Staib, "Boundary finding with prior shape and smoothness models," *IEEE Trans. on Pattern Analysis and Machine Intelligence (PAMI)*, vol. 22, no. 7, pp. 738–743, 2000.
23. J. Yang, L. H. Staib, and J. S. Duncan, "Neighbor-constrained segmentation with 3d deformable models," in *Proc. IPMI (Information Processing in Medical Imaging)*, Ambleside, UK, July 2003, pp. 198–209.
24. S. Zhu, "Embedding gestault laws in markov random fields," *IEEE trans. on PAMI*, vol. 21, no. 11, 1999.